SURFACE WAVE PROPAGATION EFFECTS OBSERVED AT THE SAUDI SEISMIC NETWORK

Gabi Laske and Nathalie Cotte

Cecil H. and Ida M. Green Institute of Geophysics and Planetary Physics, La Jolla

Sponsored by The Defense Threat Reduction Agency
Through SAIC Subcontract Number: 44000025260

ABSTRACT

Global surface wave arrival angles (also called polarization data) are extremely useful data to constrain the short-wavelength structure in global surface wave phase velocity maps. This paper investigates the feasibility of using such data on a more regional scale to validate regional models. We measure the arrival angles at the Saudi Arabian Seismic Network and compare them with predictions calculated using published phase velocity maps. We find large discrepancies between data and existing maps and demonstrate the great potential such data have to constrain the regional structure around the Saudi Arabian Peninsula. A by-product of our procedure is the retrieval of the misalignment of the horizontal components of the seismic sensor. We find a significant misalignment of approximately 4 degrees for the seismometer at station AFIF.

Key Words: Seismic Surface Waves, Western Asia, Saudi Network, Arrival Angles, Surface Wave Dispersion, Model Validation

OBJECTIVE

The objective of this research is to investigate techniques and surface wave datasets to validated regional crustal and upper mantle models. Special attention is dedicated to assess the feasibility of using arrival angle data in this process. This project concentrates on waves propagating in the area covering Western Asia, Near East, Eastern Europe and Northern Africa.

RESEARCH ACCOMPLISHED

Introduction

Under the new SAIC consortium grant DTRA01-PRDA-99-01, a group of University affiliates work with SAIC to compile a new high-resolution crust and upper mantle model for Western Asia and Northern Africa. This initiative is driven by both factors the need of the seismic monitoring community for a model that is more accurate than what is currently available and the recent vast increase of a variety of regional seismic data. While all the traditionally used databases will go into the modelling process, ranging from crustal refraction seismic data bases to dispersion measurements for short- and intermediate-period regional and semi-regional surface waves, some others will not be considered. Among these are surface wave arrival angles, also called polarization data. The reasons why such data are usually not considered in regional (and global) modelling are many-fold and include the comparably large difficulty to obtain precise measurements, the dependence on horizontal component records, the increased sensitivity to noise and the complexity of the theoretical framework to interpret the measurements.

Since polarization data are more sensitive to small-scale structure than surface wave dispersion data are, it seems natural to use such data in the validation process of a newly developed model. In this paper, we investigate the feasibility of this endeavor. While our database is routinely updated to include data from all broad-band stations available for the Western Asian and Northern African Region, the study presented here concentrates on observations obtained at the Saudi Arabian Seismic Network (Figure 1). This network was installed by colleagues Frank Vernon and Rob Mellors at Scripps (Vernon et a., 1996) and was operational from December 1995 through February 1997 (Table 1).

Report Documentation Page

Form Approved
OMB No. 0704-0188

1. REPORT DATE	2. REPORT TYPE	3. DATES COVERED
SEP 2000		**00-00-2000 to 00-00-2000**

4. TITLE AND SUBTITLE	5a. CONTRACT NUMBER
Surface Wave Propagation Effects Observed At The Saudi Seismic Network	5b. GRANT NUMBER
	5c. PROGRAM ELEMENT NUMBER
6. AUTHOR(S)	5d. PROJECT NUMBER
	5e. TASK NUMBER
	5f. WORK UNIT NUMBER
7. PERFORMING ORGANIZATION NAME(S) AND ADDRESS(ES) **University Of California,Cecil H and Ida M. Green Institute of Geophysics and Planetary Phys,La Jolla,CA,92093**	8. PERFORMING ORGANIZATION REPORT NUMBER
9. SPONSORING/MONITORING AGENCY NAME(S) AND ADDRESS(ES)	10. SPONSOR/MONITOR'S ACRONYM(S)
	11. SPONSOR/MONITOR'S REPORT NUMBER(S)

12. DISTRIBUTION/AVAILABILITY STATEMENT
Approved for public release; distribution unlimited

13. SUPPLEMENTARY NOTES
Proceedings of the 22nd Annual DoD/DOE Seismic Research Symposium: Planning for Verification of and Compliance with the Comprehensive Nuclear-Test-Ban Treaty (CTBT) held in New Orleans, Louisiana on September 13-15, 2000, U.S. Government or Federal Rights.

14. ABSTRACT
See Report

15. SUBJECT TERMS

16. SECURITY CLASSIFICATION OF:			17. LIMITATION OF ABSTRACT	18. NUMBER OF PAGES	19a. NAME OF RESPONSIBLE PERSON
a. REPORT	b. ABSTRACT	c. THIS PAGE			
unclassified	**unclassified**	**unclassified**	**Same as Report (SAR)**	**10**	

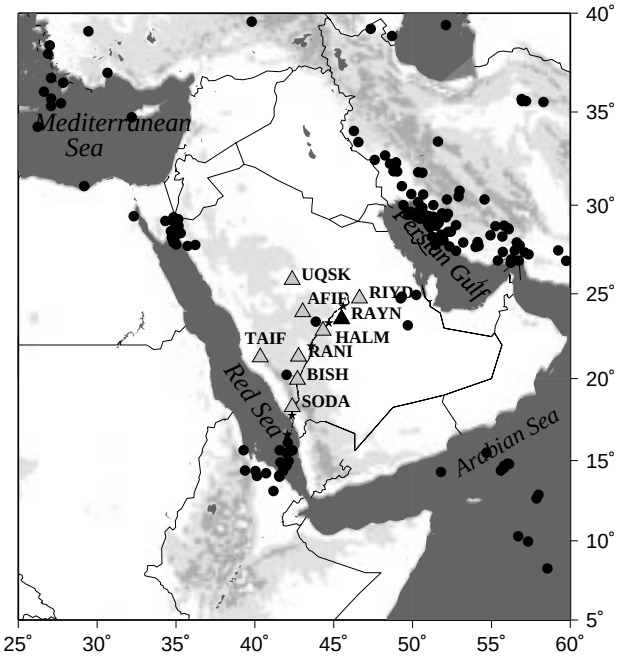

Figure 1. Map of the temporary Saudi Arabian Seismic Broadband Network (triangles). BISH was operational from November to December 1995, while station RAYN became the permanent IRIS/IDA station in June 1996 (see also Table 1). The circles are regional events recorded by the network between November 1995 and May 1996.

Table 1. The Saudi Arabian Seismic Network

Station	Latitude	Longitude	Start	End	Location
AFIF	23.9310	43.0400	95.327	97.055	Afif
BISH	19.9228	42.6901	95.322	95.338	Bisha
HALM	22.8454	44.3173	95.327	97.055	Hadabat Al-Mahri
RANI	21.3116	42.7761	95.338	97.058	Raniyah
RAYN	23.5220	45.5008	95.337	96.160	Ar Rayn
RIYD	24.7220	46.6430	96.069	97.060	Riyadh
SODA	18.2921	42.3769	95.338	97.058	Al-Soda
TAIF	21.2810	40.3490	96.158	96.240	Taif
UQSK	25.7890	42.3600	96.161	97.055	Uqlats Sakur

A useful by-product of the investigation of polarization data is the retrieval of the misalignment of the horizontal components. Significant misalignment of more than 5 degrees has been found at global broad-band stations (Laske, 1995; Laske and Masters, 1996) which has often later been confirmed and corrected by the network operators. For example, a previously unknown significant deviation of the north-component from true North could be corrected at station AAK -- a key station for the seismic monitoring community -- in January 1994 after we detected a misalignment in our dataset. In this paper, we present the misalignment of the horizontal components found for the stations of the Saudi Seismic Network.

Peculiar Waveforms in the Surface Wave Database

Our current database for the Saudi Arabian Seismic Network includes surface wave waveforms for all shallow large events (source depth less than 150 km; seismic moment greater than 4×10^{18} Nm). These events typically have surface wave magnitudes Ms=6.2 and larger. We also include smaller events (with seismic moments greater than

$5x10^{17}$ Nm) for epicentral distances smaller than 95 degrees for which the surface wave magnitudes are typically 5.2 and larger. Our database has yet to be augmented with the smaller regional events (e.g. as shown in Figure 1) but now has 176 shallow, mainly teleseismic events. The raw 40 Hz data which are available at the IRIS/DMC are initially decimated to 1 Hz data and low-pass filtered at 37 s. All 3-component records are also corrected for instrumental effects and the horizontal components are rotated into radial and transverse components. In the processed 3-component records, we often notice a surprisingly large signal on the transverse component, at the same time as the fundamental mode Rayleigh wave train but significantly later than the expected time for the fundamental mode Love wave. This is especially the case for events occurring in the Kuril Islands region (Figure 2).

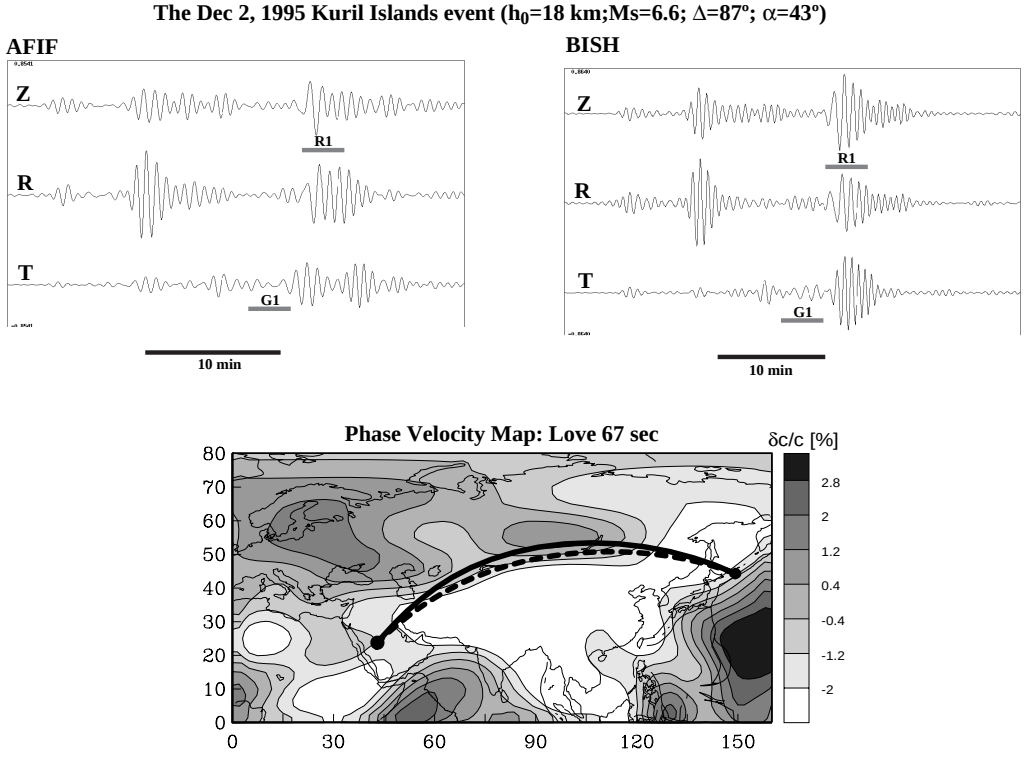

Figure 2. top: Three-component records at stations AFIF and BISH of the Dec 2, 1995 (95.336) Kurils Islands event. Note the strong signal on the transverse component at the theoretical Rayleigh wave arrival time (R1). Also note the lack of signal at the time predicted for the Love wave to arrive (G1) and the difference of signal between stations AFIF and BISH. The seismograms were low--pass filtered for periods longer than 37s.
bottom: A section from the global phase velocity map of Laske and Masters (1996) for Love waves at 67 s. Also shown is the source-receiver great circle (dashed) and the actual ray (solid) resulting from a ray tracing calculation using this map. The ray diverts up to 3 degrees from the great circle and the arrival angle predicted at the receiver is -6 degrees.

Tests with synthetic seismograms show that events in the Kuril Islands with source mechanisms similar to that of the Dec 2, 1995 event produce only little fundamental mode Love wave energy on the transverse components at the Saudi Array. We therefore suspect that the observed signal is composed of either delayed scattered Love waves or accelerated short-period Rayleigh waves that were refracted into faster regions adjacent to the great-circle path between the source and receiver. Multi-pathing effects would therefore “rotate” the seismic wave packets for Rayleigh and Love waves from the expected radial and transverse components. To test our hypothesis, we perform 2D ray tracing calculations using the phase velocity maps that are available in the literature. For estimating the effects at long and short periods we compare the calculations for the phase velocity maps of Ekstrom et al. (1997) and of Laske and Masters (1996) at different periods. The map in Figure 2 represents the "average case" around 65 s for which lateral heterogeneity diverts the ray path up to 3 degrees away from the source-receiver great circle. The arrival angle at station AFIF is about 6 degrees if looking toward the source. Lateral refraction is less at longer periods where heterogeneity is more dominated by long-wavelength structure (the arrival angle at 100 s is 2 degrees)

and gets stronger for shorter periods (the arrival angle at 35 s is 7.5 degrees). We also use the linear path integral approximation of Woodhouse and Wong (1986) to predict arrival angles. For 35 s we obtain an angle of 14.5 degrees which is significantly different from the ray tracing angle. Discrepancies of this magnitude are usually indicative for significant multi-pathing effects between source and receiver so that both theoretical values are invalid and a polarization measurement from the corresponding seismogram cannot be interpreted in terms of a wave propagating along a single ray.

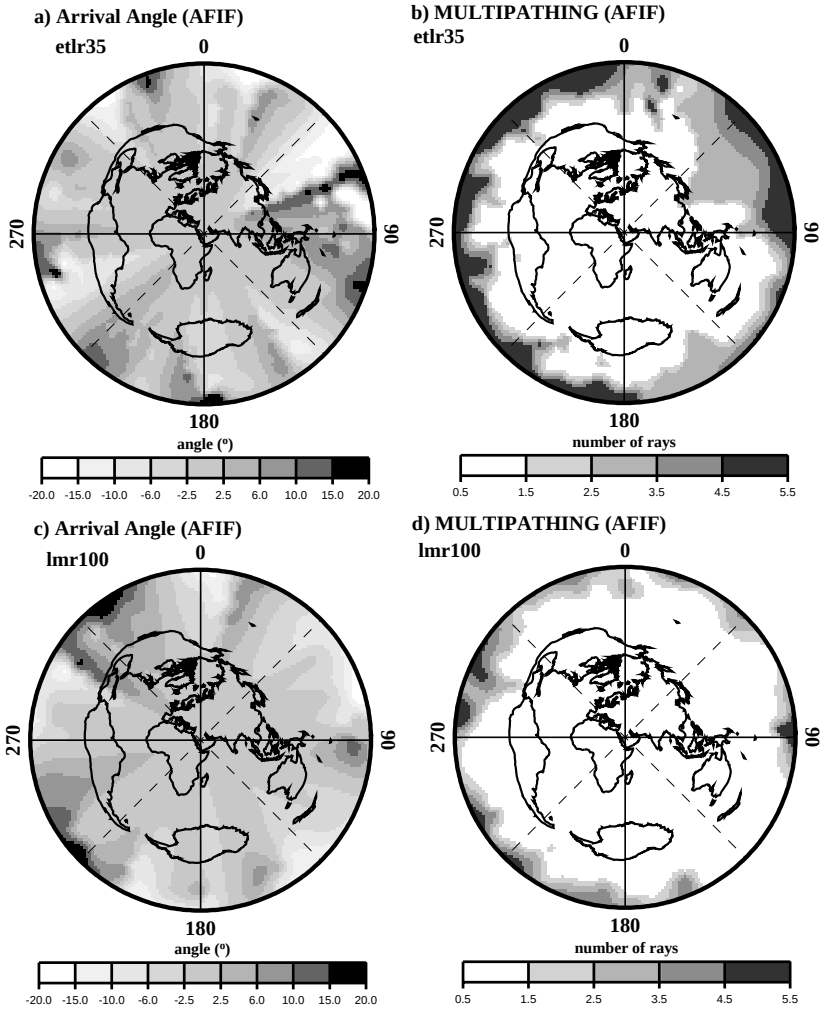

Figure 3. Ray tracing maps obtained by using the global phase velocity maps of Ekstrom et al. (1997) for 35 s (etlr35) and Laske and Masters (1996) for 100 s (lmr100). The maps are drawn in polar representation and were obtained by tracing rays from fictitious source locations on a 5x5 degree grid to station AFIF at the center. a)+c) Plotted are the ray tracing angles for models etlr35 and lmr100 obtained for each fictitious source at its source location. b)+d) Multi-pathing expressed as the number of rays arriving within less than a wave period. Considerable multi-pathing is found for events in the Kuril Islands region for short periods, while for long periods this effect as well as off-great circle arrival angles are moderate.

In Figure 3, we demonstrate the severity of multi-pathing for the case of station AFIF. We use the FD ray tracer of Farra (1990) to calculate arrival angles as well as estimate the strength of multi-pathing by counting the rays that come in at the same time within a period. Calculations are performed with fictitious sources on a 5x5 degree grid. We notice strong multi-pathing and large predicted arrival angles for fictitious events occurring near the Kuril Islands. As expected, the effect is much weaker for longer periods for which the phase velocity maps contain significantly less short-wavelength structure. From this experiment we conclude that arrival angles measured for

short periods at the Saudi Arabian Seismic network for events occurring in the Kuril Island regions cannot be used in the modelling of seismic structure.

Polarization Angles-Station Misorientation

Using the multi-taper technique of Laske et al. (1994a), we are able to obtain 384 high-precision arrival angles for 83 of the 176 events at each period between 250 and 60s and 204 angles at each period between 60 and 40s for 48 additional events. Table 2 summarizes the number of measurements for both Love and Rayleigh waves for each station and some examples of measurements are shown in Figure 4. Values at all periods are usually to within 25 degrees of the great circle direction but the variance in the data increases significantly as periods get shorter (not shown). The observed arrival angles at station AFIF are peculiar. For both Love and Rayleigh wave the angles concentrate around -5 degrees. Less strong but also obvious is a similar clustering of the data at station SODA. The relative stability of these mean values may encourage the data analyst to adopt them as an underlying misrotation of the horizontal components. However, some contribution to the mean in the data may come from lateral heterogeneity. This is especially true for stations with only few measurements. In order to avoid mapping component misalignment into seismic heterogeneity and vice versa we prefer to include a component misalignment as additional model parameters in a joint inversion for structure (Laske, 1995). The relationship between polarization angles and component misalignment is non-linear but can easily be linearized and solved for in an iterative procedure in which only 1 or 2 iterations are necessary for the system to converge. The joint inversion of the new polarization data observed at the Saudi Network is performed with the augmented global database of Laske and Masters (1996), for long-wavelength structure up to harmonic degree 12. To increase the accuracy of the determined component-misalignment, we perform similar inversions for at least 6 cases which are typically 3 periods in the long-period band (250-100s) for both Rayleigh and Love waves and then average the results. We use only long periods because the increasing contribution from short-wavelength structure could induce a bias at shorter periods, especially for stations with uneven data coverage.

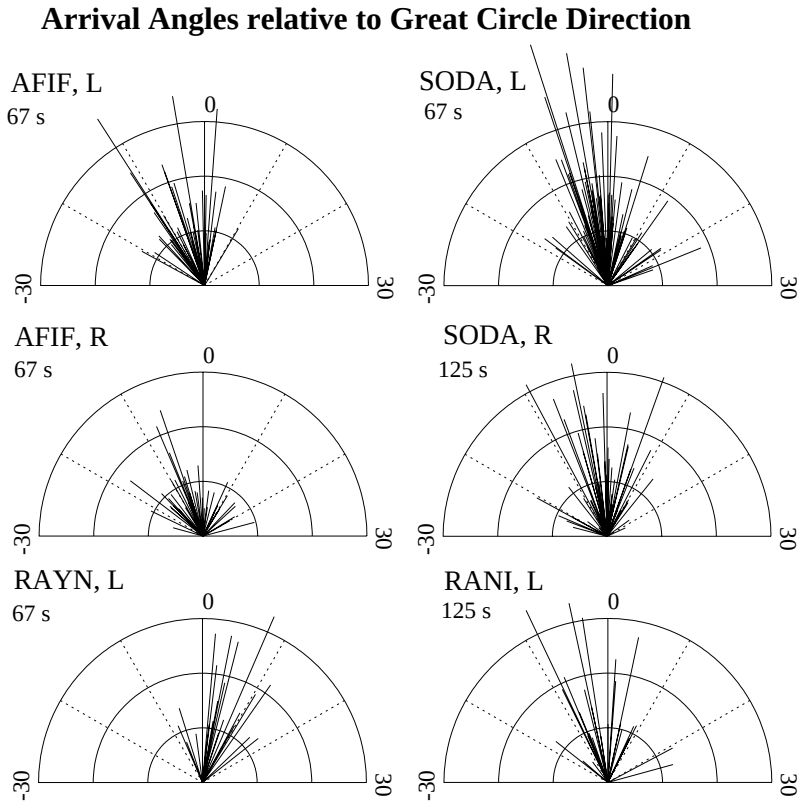

Figure 4. Polarization angles at stations AFIF, SODA, RAYN and RANI for Rayleigh (R) and Love (L) waves at 67 s and 125 s period. The plots show rose diagrams, where the polar angle is the off-great circle arrival angle and the

length of the plotted vector is the reciprocal error bar. Accurate measurements with small error bars tend to stick out of the cluster of observations. At stations AFIF, many of the measurements cluster at about -5 degrees. This is observed for both Love and Rayleigh waves at all frequencies. The horizontal components at this site were likely to be misaligned.

Table 2. Component Misalignment Expressed as Apparent North

Station	# Rayleigh	# Love	Apparent North [deg]	Comment
AFIF	64	57	-4.22 +/- 0.66	
BISH	5	5	0.52 +/- 1.35	uncertain; stolen after 2 weeks
HALM	35	38	-1.65 +/- 0.84	
RANI	34	35	-2.76 +/- 0.96	
RAYN	29	25	1.71 +/- 0.87	
RIYD	5	14	0.70 +/- 1.34	uncertain; late installation
SODA	83	93	-2.72 +/- 0.54	
TAIF	16	18	-4.01 +/- 1.66	uncertain; late installation
UQSK	15	17	-4.04 +/- 2.52	uncertain; late installation

Table 2 summarizes the component misalignment that we obtain for the stations of the Saudi Network. Though the of amount of data at each station is relatively low as compared to those for permanent broad-band stations of the global seismic network, we obtain stable results at at least 4 of the 9 stations (AFIF, RANI, RAYN and SODA). Note that the components at station AFIF are significantly rotated with respect to true North by approximately 4 degrees. Stations SODA and RANI also have significant misalignment though it is smaller than at station AFIF. The misalignment at these three stations implies that the systems are rotated clockwise from true North, while the components at RAYN are rotated anti-clockwise. The number of data at stations BISH, RIYD and TAIF is relatively low which is reflected in the larger error bar for the misalignment. However, the misalignment at station TAIF is at least 2.5 degrees. The value for station UQSK is somewhat uncertain as the few available measurement have large error bars and Love and Rayleigh wave angles seem inconsistent. It is important to recognize that the polarization data have to be corrected for component misalignment in these cases as predictions using existing high-resolution global phase velocity maps are typically within 5 degrees from the source-receiver great circle, hence of the same magnitude.

Polarization Angles -- Compatibility with Existing Dispersion Maps

After the polarization data have been corrected for component misalignment, the data can now be used to validate an existing model or be used jointly with other data in an inversion for a new model. To test whether the data are consistent with currently existing models, we compare the arrival angles at various periods with the predictions calculated for a particular phase velocity map. We chose the linear path integral approximation of Woodhouse and Wong (1986) as theoretical framework to interpret the measured arrival angles as an integral of the transverse gradient of phase velocity perturbation along the source-receiver great circle. The phase velocity maps we test are those of Laske and Masters (1996) (L&M), Ekstrom et al. (1997) (ET&L), Trampert and Woodhouse (1995) (T&W) and their updated version (Trampert and Woodhouse, 1996). All maps are available on the WWW or through anonymous ftp and are expanded in surface spherical harmonics where the truncation level varies. The L&M maps are expanded up to l=24, while the maps of ET&L and T&W are truncated at l=36 or l=40. We find that the short-wavelength structure in the ET&L and T&W maps for harmonic degree 25 and above generally increases the misfit of the data so we truncate all maps for the comparison in Table 3 at l=24, while maintaining the original truncation in Figure 5. We should also note that the linear theoretical framework to interpret polarization data starts to break down if significant large-amplitude structure at l=36 is present (Laske et al., 1994b; Wang and Dahlen, 1995). We find that the different maps for similar periods can give very different variance reductions though the maps look rather similar (Table 3, Figure 5). For example, our polarization data are reasonably consistent with the T&W Rayleigh wave phase velocity maps at 100 and 67 s but are clearly inconsistent with the Love wave maps of the same authors. It is

interesting to note that the updated version of 1996 fairs much worse than the 1995 version, possibly due to the fact that the 1996 maps contain more incompatible short-wavelength structure (l=10-24) than the 1995 maps. Our polarization data are also inconsistent with the L&M maps. We can achieve a significantly better fit to the data with variance reductions up to 40% when we include the new data in a joint inversion with the global polarization and dispersion dataset of Laske and Masters (1996) for new phase velocity maps. An example is shown in Figure 5.

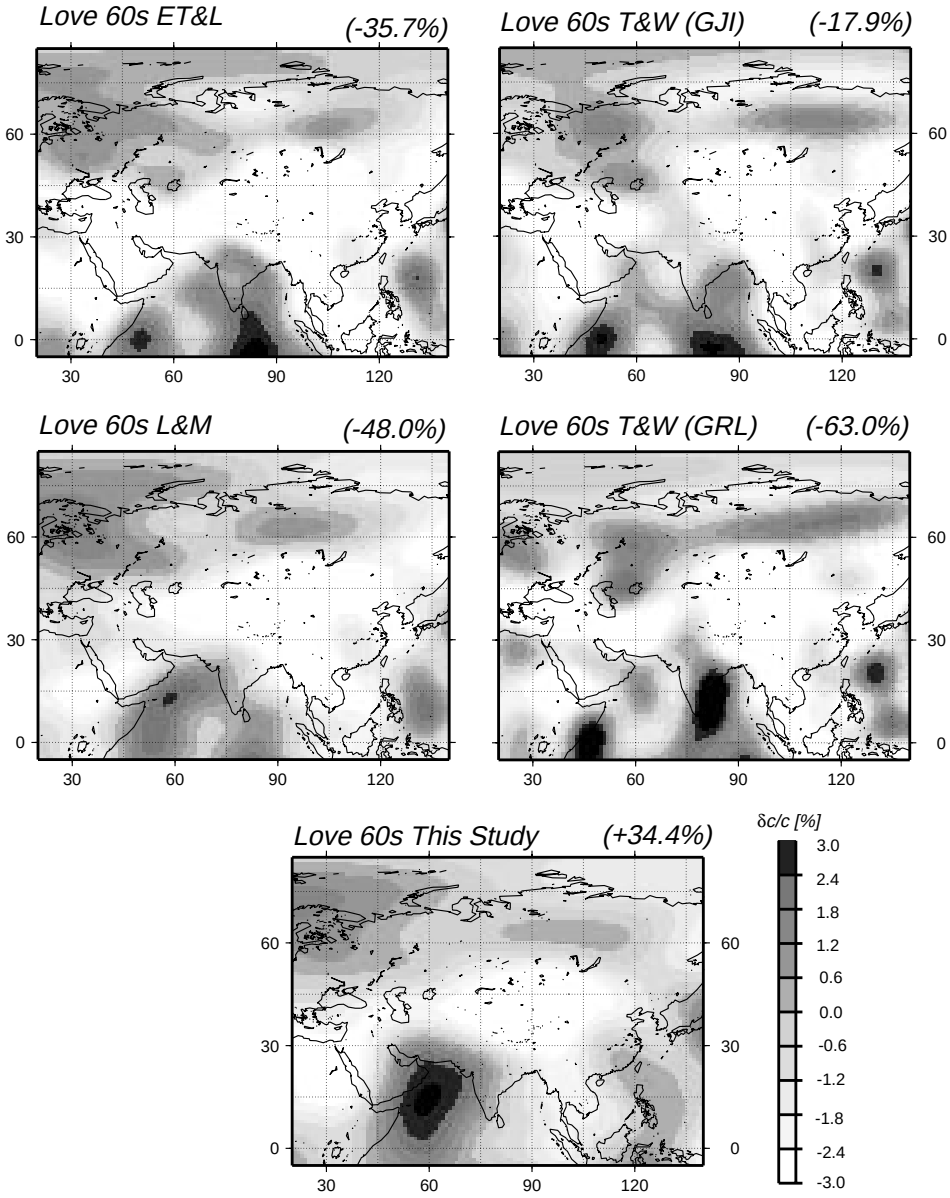

Figure 5. Sections of the global phase velocity maps of Ekstrom, Tromp and Larson (1997) (ET&L), Trampert and Woodhouse (T&W; 95=GJI; 96=GRL) and Laske and Masters (1996) for Love waves at 60 sec (L&M). All maps are expanded in surface spherical harmonics, with different truncation levels (ET&L: l=36; T&W: l=40; L&M: l=24). The lower panel shows a map obtained from a joint inversion of the L&M dataset and the new arrival angle data of the Saudi Seismic Network. Note that the new data require significant changes in regional structure to be well fit (the number in the right upper corners list the variance reduction for each map).

Obviously, the new data require a significant enhancement of structure to the southeast of the Saudi Arabian Peninsula. Also note that changes in the model can occur as far the Philippines. We want to stress that the data

coverage of the L&M dataset is significantly poorer than that of the ET&L dataset (about 1/3) and that the map shown in Figure 5 should not be regarded as a new model for the Eurasian region. We are also currently measuring arrival angles across the array using a wavefront fitting technique that was successfully applied to intermediate-period data recorded in the French Alps (Cotte et al., 2000). A possible discrepancy with the polarization data introduced in this paper could point either toward the complexity of the approaching wavefront, inconsistencies in the polarization dataset and local anisotropy. Obviously, this project is ongoing research but we want to summarize by pointing out the great potential of a dataset of high-precision polarization measurements to constrain structure on a regional scale.

Table 3. Variance Reduction for the Saudi Polarization Data

Data Type	L&M	ET&L	T&W 95	T&W 96
R 150s	6	13	21	-2
R 100s	-17	20	29	23
R 67s	-62	-6	24	28
R 50s	0	-10	-	-
R 40s	-	-5	-21	-27
L 150s	-9	-6	-15	-53
L 100s	-44	-5	-4	-42
L 67s	-48	-36	-18	-63
L 50s	12	9	-	-
L 40s	-	2	1	-36

CONCLUSION AND RECOMMENDATIONS

We have described our current catalog of arrival angle measurements (also called polarization data) at the Saudi Arabian Seismic Network and we have demonstrated the great potential of such a dataset for

a) re-calibrating the orientation of horizontal components

b) validating existing models using such data

While sifting our database for outliers we produced ray tracing maps for stations at the Saudi Network. Such maps are invaluable tools to identify source regions that are likely to be the origin of travel paths that suffer from severe multi-pathing effects, for a given station. Not only should polarization measurements for such events be discarded a priori as outliers. Dispersion measurements, especially measurements of group travel time can also strongly be affected by distortions in the spectral amplitudes that are caused by focusing-defocusing effects. For the case of the Saudi Arabian Seismic Network, we should obviously discard all polarization data for events occurring in the Kuril Islands region and we should also investigate the consistency of dispersion measurements for the corresponding seismic records very carefully when modelling Earth structure or locating events.

It is important to realize that the ray tracing maps vary strongly from station to station within the Western Asian/Northern African region and also vary as a function of period. We typically identify less critical source regions for longer periods (about 100s) than for shorter periods (35s) since longer period surface waves are less affected by relatively shallow (i.e crustal) short-wavelength structure. A particular source region may display multi-pathing for one station but not for another. For example, waveforms recorded for the Kuril Islands events that were so peculiar for the Saudi Array will most likely not suffer from multi-pathing effects at IRIS/IDA stations AAK and ABKT as indicated in Figure 6. On the other hand, Macquarie Ridge events will likely produce distorted short-period surface wave packets at station AAK. The same is true for events in the Solomon/Fiji/Tonga subduction system recorded at station ABKT. Also worth mentioning is the fact that multi-pathing can occur for events significantly closer than 90 degrees, an epicentral distance cut-off that is typically used in regional surface wave tomography. We therefore recommend to

c) produce ray tracing maps for individual stations to evaluate a potential bias in surface wave polarization and dispersion data caused by focusing-defocusing effects.

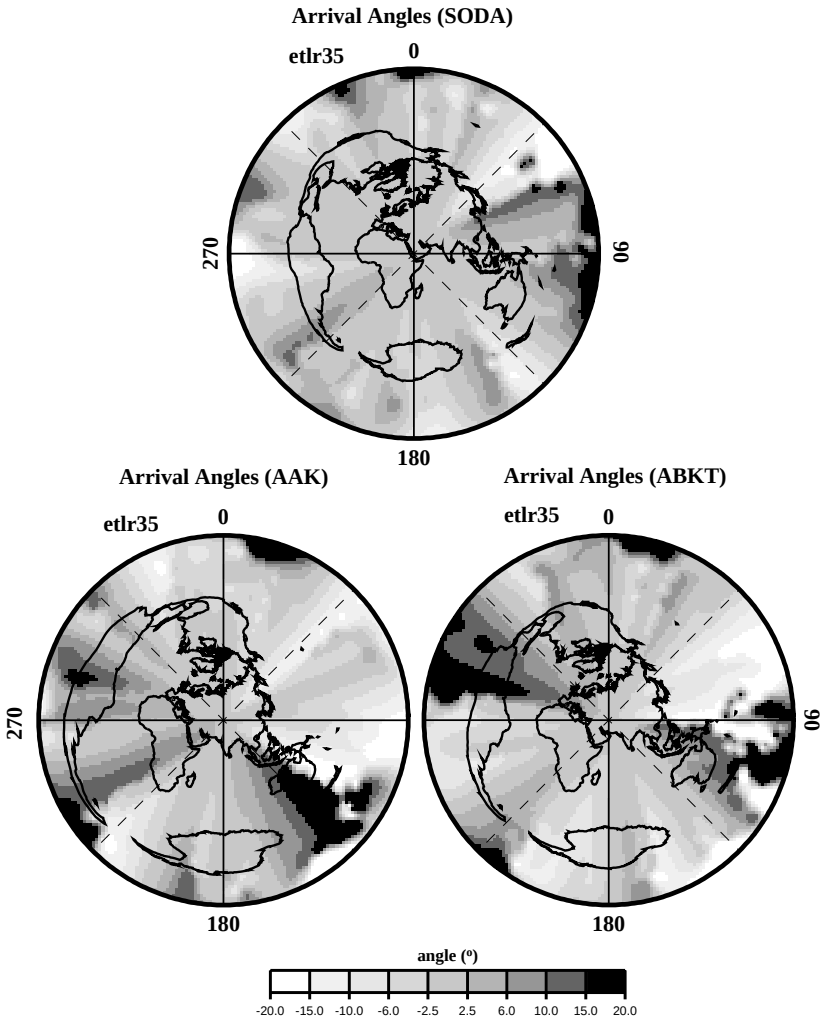

Figure 6. Ray tracing maps obtained with global phase velocity maps of Ekstrom et al. (1997) for 35 s (etlr35) for the Saudi Seismic station SODA and the IRIS/IDA stations AAK and ABKT. For details see Figure 3. Note that the maps look quite different for the relatively close stations AAK and ABKT.

REFERENCES

Cotte N., Pedersen H.A., Campillo M., Farra V. and Cansi Y., 2000. Off-great circle propagation of intermediate period surface waves as observed on a dense array in the French Alps, *Geophys. J. Int*., in press.

Ekstrom, G., J. Tromp, and E.W. Larson, 1997. Measurements and models of global models of surface wave propagation, *J. Geophys. Res*., **102**, 8137—8157.

Farra, V., 1990. Amplitude computation in heterogeneous media by ray perturbation theory: a finite element approach, *Geophys. J. Int*., **103**, 341—354.

Laske, G., G. Masters, and W. Zurn, 1994a. Frequency-dependent polarization measurements of long-period surface waves and their implications for global phase-velocity maps, *Phys. Earth Planet. Int*., **84**, 111-137.

Laske, G., G. Masters, and J. Um, 1994b. Phase, amplitude and polarization of surface waves and the fine-scale structure of global dispersion maps, *EOS Trans. AGU*, **75**, F 476.

Laske, G., 1995. Global observation of off-great circle propagation of long-period surface waves, *Geophys. J. Int.*, **123**, 245—259.

Laske, G., and G. Masters, 1996. Constraints on global phase velocity maps by long-period polarization data, *J. Geophys. Re*s., **101**, 16,059--16,075.

Trampert, J., and J.H. Woodhouse, 1995. Global phase velocity maps of Love and Rayleigh waves between 40 and 150 seconds, *Geophys. J. Int*., **122**, 675—690.

Trampert, J., and J.H. Woodhouse, 1996. High-resolution global phase velocity distribution, *Geophys. Res. Let.*, **23**, 21—24.

Vernon, F., R.J. Mellors, J. Berger, A.M. Al-Amri, and J. Zollweg, 1996. Initial results from the deployment of broad-band seismometers in the Saudi Arabian Shield, *Proceedings of the 18th Seismic Research Symposium on Monitoring a Comprehensive Test Ban Treaty*, 4-6 Sept, Annapolis, Maryland, 108—117.

Wang, Z., and F.A. Dahlen, 1995. Spherical-spline parameterization of three-dimensional Earth models, *Geophys. Res. Lett*., **22**, 3099—3102.

Woodhouse, J.H., and Y.K. Wong, 1986. Amplitude, phase and path anomalies of mantle waves, *Geophys. J. R. Astron. Soc*., **87**, 753—773.